Chapter 5

Infrared Spectra and Density Functional Theoretical Calculation of Transition Metal Oxide Reaction with Monochloromethane

Yanying Zhao, Xin Liu and Shuang Meng

Additional information is available at the end of the chapter

http://dx.doi.org/10.5772/64437

Abstract

In this chapter, we presented a short review of past and present experimental and theoretical work on the reactions of the transition metal monoxide and dioxide molecules with monochloromethane in excess argon matrices. A series of infrared absorption spectra combining with density functional theoretical (DFT) calculation characterized that the transition metal monoxide molecules produced by laser-ablated higher oxides activated C—H and C—Cl bonds of CH_3Cl to first form the weakly bound $MO(CH_3Cl)$ (M = Sc, Y, Nb, Ta, Ti, Zr, Mn, Fe) complexes, which further photoisomerized to the more stable chlorine-transfer (Cl-transfer) CH_3OMCl (M = Sc, Y), $CH_3M(O)Cl$ (M = Ti, Zr), CH_3MOCl (M = Mn, Fe), and agostic hydrogen-transfer (H-transfer) CH_2ClMOH (M = Sc, Y, Nb, Ta) products upon limited light excitation. Transition metal dioxides reaction with CH_3Cl also formed $MO_2(CH_3Cl)$ (M = Ti, Zr, Nb, Ta) complexes, which were further rearranged to the more stable Cl-transfer $CH_3OM(O)Cl$ (M = Ti, Zr) and agostic H-transfer $CH_2ClM(O)OH$ (M = Nb, Ta) molecules between the metal center atom and the chlorine atom upon ultraviolet light irradiation. Their different reactivity was interpreted according to the different valence electrons of metal center.

Keywords: monochloromethane, chlorine transfer, hydrogen transfer, transition metal oxides, agostic interaction

1. Introduction

Monochloromethane, as the one of the simplest halohydrocarbons, also called methyl chloride, plays an important role in the industrial, synthetic, materials chemistry. It is always regarded

that monochloromethane is the largest natural source of ozone-depleting chlorine compounds and accounts for about 15% of the present atmospheric chlorine content as one kind of chlorinated volatile organic compounds (CVOCs). At present, monochloromethane is observed in the dry leaf with the content of 0.1–0.3 μg/g/h, and large emissions of monochloromethane are observed from some common certain types of ferns and dipterocarpaceae [1, 2]. Monochloromethane is also industrially produced by the oxidation and chlorination reaction of methane in the presence of metal chloride catalyst, and drying monochloromethane conversed to gasoline and olefins on the methanol to gasoline (MTG) and the methanol to olefins (MTO) catalysts [3, 4]. The conversion of methyl chloride to hydrocarbons has been investigated since the mid-1980s [5]. The product distribution of methyl chloride to hydrocarbons is strikingly similar to methanol conversion over the same topology [6]. Recently several ZSM-5 zeolites and SAPO sieves catalysts were reported the high performances on the catalytic conversion of monochloromethane to light olefins [7–9]. Modified SAPO-34 catalysts were also chosen to enhance its catalytic performance for the conversion of chloromethane to light olefins [10–13]. The oxidation addition of metal into carbon-halogen bonds is a key step in many stoichiometric and catalytic reactions. Activation of compounds containing C—X (X = Cl, Br, I) bonds attracts widespread interest due to the underactive organic functional group and the inherent chemical properties. Predominantly alkyl and aryl halides are extensively applied as electrophiles in the transition metal-catalyzed cross-coupling reactions [14–16]. It has a far-reaching significance on carbon-chlorine (C—Cl) bond catalytic oxidation on the conversion of monochloromethane to gasoline and olefins.

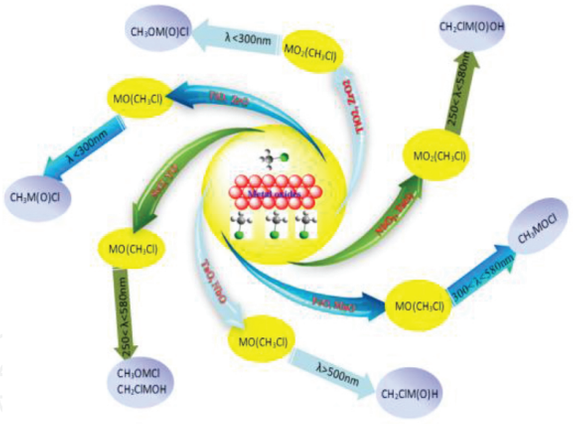

Scheme 1. The reactivity of transition metal monoxide and dioxide with monochloromethane in argon from Refs. [27–30].

The reactions of transition metal centers with chloromethane may serve as the simplest model for understanding the intrinsic mechanism of the organic halides catalytic oxidation processes. The reactions on transition metal atoms with monochloromethane have been intensively studied in solid noble gas matrices. Investigations have reported that C—X bond of CH_3X (X = F, Cl, Br, I) are activated by transition metal atoms [17–22]. The higher valence of group 6 metals can form the methylidyne complexes CH = MH_2X (M = Mo, W, X = H, F, Cl, Br) [23–26]. In this chapter, the reactions of simple transition-metal oxide molecules with monochloromethane in

http://dx.doi.org/10.5772/64437

solid argon were reviewed using matrix infrared absorption spectroscopy and density functional theoretical (DFT) calculations. As shown in **Scheme 1**, the ground-state transition metal monoxide molecules activated carbon-hydrogen (C—H) and C—Cl bond of CH_3Cl upon a certain wavelength excitation in argon matrices. The weakly bound $MO(CH_3Cl)$ (x = 1, 2; M = Sc, Y, Nb, Ta, Ti, Zr, Mn, Fe) complexes were initially formed and then isomerized to the more stable Cl-transfer CH_3OMCl (M = Sc, Y) and $CH_3M(O)Cl$ (M = Ti, Zr, Nb, Ta, Mn, Fe), and agostic H-transfer CH_2ClMOH (M = Sc, Y, Nb, Ta) isomers upon limited visible light excitation. The $MO_2(CH_3Cl)$ (M = Ti, Zr, Nb, Ta), which were formed from the reactions on MO_2 with CH_3Cl, were further rearranged to the more stable Cl-transfer $CH_3OM(O)Cl$ (M = Ti, Zr) and H-transfer $CH_2ClM(O)OH$ (M = Nb, Ta) molecules with agostic interactions between the chlorine and the metal center under ultraviolet light irradiation.

2. Experimental and computational methods

The experimental setup for pulsed laser-ablated and matrix isolation Fourier transform infrared (FTIR) spectroscopic technique has been previously described in detail [31]. Briefly, the 1064 nm Nd:YAG laser fundamental (Spectra Physics, DCR 150, 20 Hz repetition rate, and 8 ns pulse width) was focused onto the rotating bulk metal oxide targets, which were prepared by sintered metal oxide powders. Laser-evaporation of bulk higher metal oxide targets has been proved to be an extensively available technique to prepare pure metal oxides in noble gas matrices [32–34]. Using standard manometric technique, the CH_3Cl/Ar samples were mixed at a proper proportion in a stainless steel vacuum line. The CH_3Cl sample was subjected to several freeze-pump-thaw cycles at 77 K before use. The laser-evaporated species were co-deposited with chloromethane in excess argon onto a CsI window cooled normally to 6 K by a closed-cycle helium refrigerator (ARS, 202N). The matrix samples were deposited at a rate of approximately 5 mmol/h for 1–2 h. Isotopic-labeled $^{13}CH_3Cl$ and CD_3Cl (ISOTEC, 99%) were used without further purification. Infrared spectra between 450 and 4000 cm^{-1} were recorded on a Bruker IFS 66v/s spectrometer using HgCdTe (MCT) detector cooled by liquid N_2 at 0.5 cm^{-1} resolution. Samples were annealed to different temperatures and cooled back to 6 K to acquire the spectra, and selected samples were subjected to visible or broadband irradiation using a 250 W high-pressure mercury arc lamp with selected wavelength glass filters.

Density functional theoretical calculations were performed by using Gaussian 03 programs [35] to identify the experimental assignments. The three-parameter hybrid functional, according to Becke with additional correlation corrections from Lee, Yang, and Parr (B3LYP), was utilized [36, 37] to optimize ground geometries, calculate frequencies, and derive the zero-point vibrational energies. Transition-state optimizations were performed with the Berny geometry optimization algorithm at the B3LYP level. The 6-311++G(d, p) basis set was used for the H, C, O, Cl, Sc, Ti, Mn, and Fe atoms [38, 39], DGDZVP basis set for Y, Zr, and Nb atoms [40, 41], and the scalar-relativistic SDD pseudopotential and basis set for Ta atom [42, 43]. In addition, the CCSD(T) method was also applied to accurately calculate the single-point energies of the B3LYP-optimized structures with the same basis sets [44].

3. Transition metal monoxides reaction with CH_3Cl

Reaction of transition metal monoxides (ScO, YO, TiO, ZrO, NbO, TaO, MnO, FeO) with monochloromethane was investigated in solid argon by infrared absorption spectroscopy, combining with isotopic substituted experiments and theoretical calculations. The initial reaction step is the formation of the $MO(CH_3Cl)$ (M = Sc, Y, Ti, Zr, Nb, Ta, Mn, Fe) complex with metal atom bound with chlorine atom and/or oxygen atom with H atoms on annealing. Upon a certain wavelength photolysis, the $MO(CH_3Cl)$ complex was isomerized by the insertion of the M═O to C─H and/or C─Cl/Cl─C bond. Selected region of infrared spectra is illustrated in **Figures 1**–**4**.

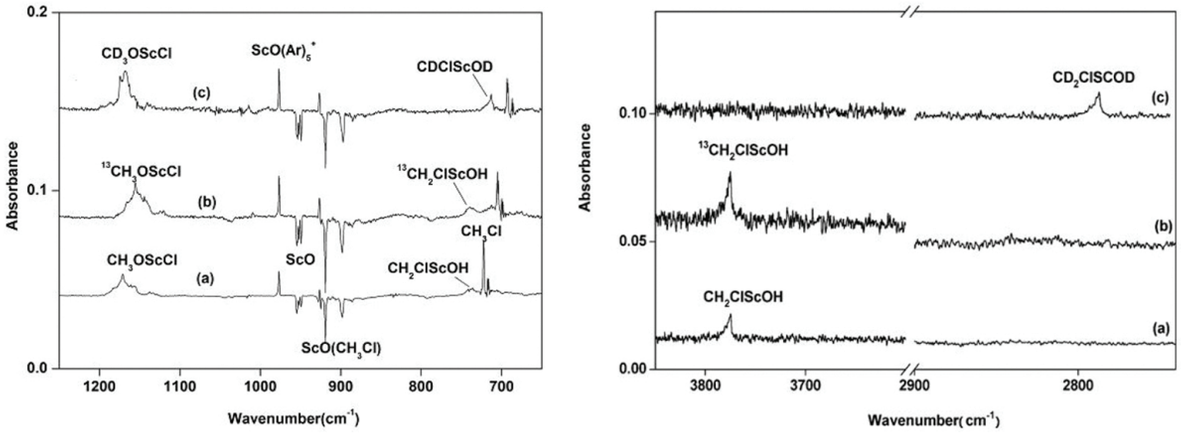

Figure 1. Difference spectra in the selected regions scandium monoxide with isotopic substituted chloromethane in excess argon. (Spectrum taken after 15 min of broadband irradiation minus spectrum taken after 25 K annealing). (a) 0.5% CH_3Cl, (b) 0.5% $^{13}CH_3Cl$, and (c) 0.5% CD_3Cl. (Reprinted with the permission from Ref. [27]. Copyright 2013 American Chemical Society).

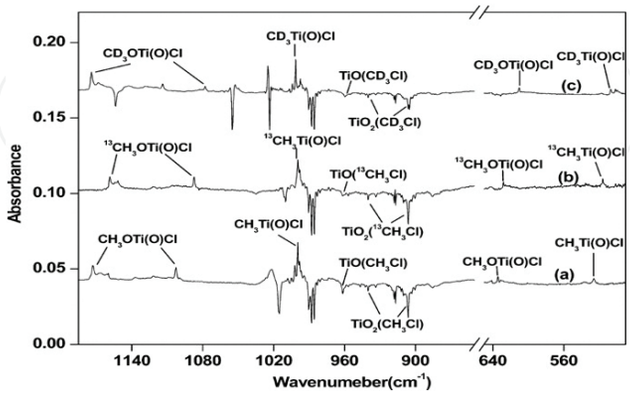

Figure 2. Difference spectra in the selected regions from co-deposition of a laser-ablated TiO_2 target in excess argon. Spectrum taken after 15 min of full-arc broadband photolysis irradiation (λ < 300 nm) followed by the 25 K annealing minus spectrum taken after sample annealing at 25 K. (a) 0.5% CH_3Cl, (b) 0.5% $^{13}CH_3Cl$, and (c) 0.5% CD_3Cl. (Reprinted with the permission from Ref. [28]. Copyright 2013 American Chemical Society).

http://dx.doi.org/10.5772/64437

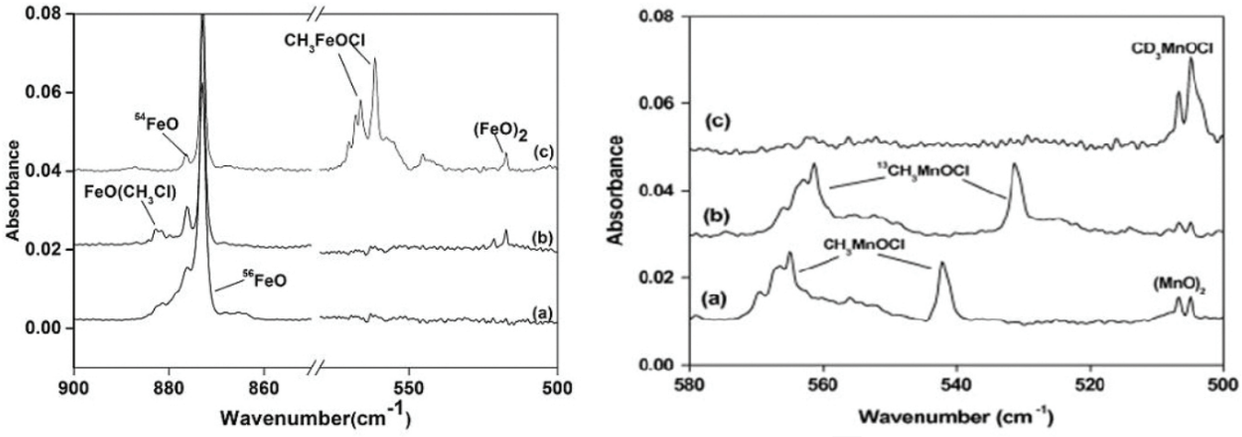

Figure 3. Infrared spectra in the selected region from co-deposition of laser-ablated MnO_2 and Fe_2O_3 target with isotopically substituted CH_3Cl in excess argon. Spectra were taken after 1.5 h of sample deposition followed by 25 K annealing and 15 min of irradiation ($300 < \lambda < 580$ nm) and 25 K annealing. (a) 0.5% CH_3Cl, (b) 0.5% $^{13}CH_3Cl$, and (c) 0.5% CD_3Cl. (Reprinted with permission from Ref. [30]. Copyright 2013, with permission from Ref. [28] from Elsevier).

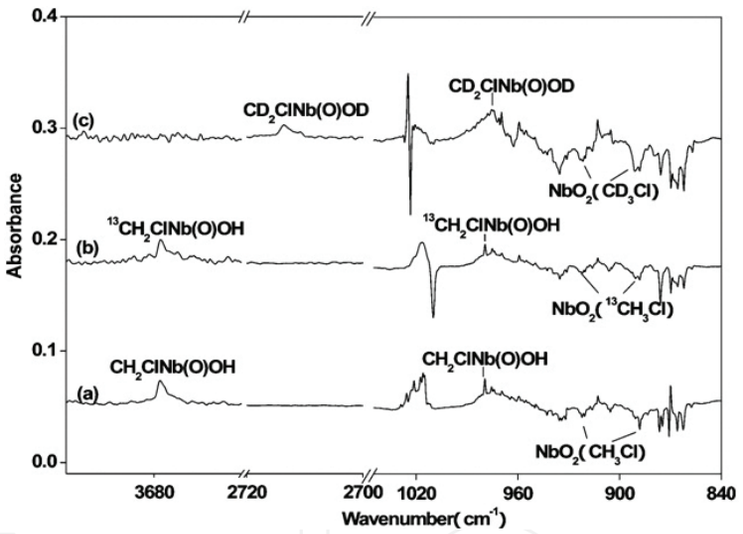

Figure 4. Difference spectra in the selected regions from co-deposition of laser-evaporated niobium oxides with isotopic-substituted monochloromethane in excess argon. Spectrum taken after 15 min of full-arc photolysis minus spectrum taken after sample annealing at 25 K. (a) 0.5% CH_3Cl, (b) 0.5% $^{13}CH_3Cl$, and (c) 0.5% CD_3Cl. (Reprinted with the permission from Ref. [29]. Copyright 2013 American Chemical Society).

In both the scandium and yttrium experiments, two $MO(CH_3Cl)$ (M = Sc, Y) complex isomers were formed spontaneously on annealing [27]. These absorptions of $MO(CH_3Cl)$ (M = Sc, Y) complex are observed at 898.4 and 919.1 cm^{-1} for Sc, and 1050.9, 805.9, and 784.8 cm^{-1} for Y, as shown in **Table 1**, which are corresponding to the Sc—O and Y—O vibration frequencies. The CH_3OMCl and CH_2ClMOH (M = Sc, Y) molecules were produced from the weakly bound $MO(CH_3Cl)$ complexes through photoinduced isomerization reactions on 250–300 nm wavelength irradiation, as shown in **Figure 1**. The CH_3OMCl (M = Sc, Y) isomer observed at

1171.5 and 565.6 cm^{-1} for Sc and 1149.2 and 490.9 cm^{-1} for Y can be regarded as being formed through the addition of the C—Cl bond to the O═M bond, whereas the CH_2ClMOH (M = Sc, Y) isomer observed at 3775.0 and 738.4 for Sc, and 3774.2 and 627.6 for Y is formed through the addition of the C—H bond to the M═O bond. On the basis of DFT calculations, the $MO(CH_3Cl)$ (M = Sc, Y) complex with C_s structure is more stable than the complex with C_{3v} structure by 25.5 (Sc) or 24.0 (Y) kJ/mol. Both CH_3OMCl and CH_2ClMOH (M = Sc, Y) molecules are more stable than the $MO(CH_3Cl)$ complex isomers. The CH_3OMCl (M = Sc, Y) molecule was predicted to proceed through a transition state with an energy barrier of 17.7 for Sc and 8.4 kJ/mol for Y from the $MO(CH_3Cl)$ complex, whereas the CH_2ClMOH isomer also proceeded through a transition state with a much higher energy barrier of 160.1 for Sc and 178.5 kJ/mol for Y from the $MO(CH_3Cl)$ complex. The CH_3OMCl (M = Sc, Y) structure is about 173.0 for Sc and 180.6 kJ/mol for Y lower in energy than the $CH_2ClScOH$ and CH_2ClYOH isomer. The CH_2ClMOH (M = Sc, Y) molecule was also calculated to involve agostic interaction observed between the metal atom and the chlorine atom due to short bond distances of 2.598 Å for Sc—Cl and 2.821 Å for Y—Cl. Such interaction is quite similar to the agostic interactions generally defined to characterize the distortion of an organometallic moiety, which brings an appended C—H bond into close proximity with the metal center [17, 21, 45].

Molecule	Ground state	Point group	Vibrational frequency[b]	Binding energy[c]	Ref.
$ScO(CH_3Cl)$	$^2A'$	C_s	898.4	−34.9	[27]
	$^2A_1$	C_{3v}	919.1	−9.4	
$YO(CH_3Cl)$	$^2A'$	C_s	1050.9, 783.5	−37.0	[27]
	$^2A_1$	C_{3v}	805.9	−13.0	
$TiO(CH_3Cl)$	$^3A'$	C_s	961.8	−41.4	[28]
$ZrO(CH_3Cl)$	^3A	C_1	898.2	−40.5	[28]
$NbO(CH_3Cl)$	$^4A'$	C_s	935.6	−29.5	[29]
$TaO(CH_3Cl)$	^2A	C_1	991.5	−5.0	[29]
$MnO(CH_3Cl)$	$^6A'$	C_s	843.4	−38.9	[30]
$FeO(CH_3Cl)$	$^5A'$	C_s	882.7	−97.4	[30]

[a] Only the values for the most abundant metal isotope are listed.
[b] The mode assignments of the experimental vibrational frequencies are discussed in the cited literature.
[c] Relative to the energy sum of ground metal oxide and CH_3Cl.

Table 1. Ground electronic states, symmetry point groups, vibrational frequencies (cm^{-1}) and binding energies (kJ/mol) for the $MO(CH_3Cl)$ species in solid argon[a].

For IVB metal monoxides, the ground-state $MO(CH_3Cl)$ (M = Ti, Zr) complexes correlate to the ground-state TiO ($^3\Delta$) and ZrO ($^1\Sigma^-$). The binding energies are predicted to be 20.5 (Ti) and 12.2 kcal/mol (Zr), which are larger than the corresponding values of $TiO(CH_4)$ and $ZrO(CH_4)$ [45, 46]. The $MO(CH_3Cl)$ (M = Ti, Zr) complexes can rearrange to the $CH_3M(O)Cl$ isomers by metal terminal insertion to C—Cl bond upon UV light irradiation (λ < 300 nm), which are

http://dx.doi.org/10.5772/64437

observed at 999.5 and 526.2 cm^{-1} for Ti, and 915.2 and 488.3 cm^{-1} for Zr, as shown in **Figure 2**. Theoretical calculations also indicated that the electronic state crossings exist from the MO (M = Ti, Zr) + CH_3Cl reaction to the more stable $CH_3M(O)Cl$ molecules through the $MO(CH_3Cl)$ complexes traverse their corresponding transition states. The $CH_3M(O)Cl$ (M = Ti, Zr) molecule was predicted to have a singlet ground state without symmetry. According to CCSD(T) single-point calculations on B3LYP optimization geometry, the singlet ground state is 44.3 kcal/mol for $CH_3Ti(O)Cl$ and 52.2 kcal/mol for $CH_3Zr(O)Cl$ lower in energy than its corresponding triplet state. The triplet $MO(CH_3Cl)$ (M = Ti, Zr) isomerized to the singlet $CH_3M(O)Cl$ (M = Ti, Zr) molecule through their corresponding transition states, which indicated that these reactions related to the spin crossing under UV light irradiation.

Molecule	Ground state	Point group	Vibrational frequency[b]	Binding energy[c]	Ref.
CH_3OScCl	^2A	C_1	1171.5, 565.6	−268.8	[27]
$CH_2ClScOH$	^2A	C_1	3775.0, 738.4	−95.8	[27]
CH_3OYCl	^2A	C_1	1149.2, 490.9	−300.3	[27]
CH_2ClYOH	^2A	C_1	3774.2, 627.6	−119.7	[27]
$CH_3Ti(O)Cl$	^1A	C_1	999.5, 526.2	−324.1	[28]
$CH_3Zr(O)Cl$	^1A	C_1	915.2, 488.3	−349.0	[28]
$CH_2ClNb(O)H$	^2A	C_1	1698.0, 985.0	−136.7	[29]
$CH_2ClTa(O)H$	^2A	C_1	1760.0, 984.8	−182.7	[29]
CH_3MnOCl	^6A	C_1	569.6, 542.2	−55.2	[30]
CH_3FeOCl	^5A	C_1	570.4, 561.5	−50.2	[30]

[a] Only the values for the most abundant metal isotope are listed.
[b] The mode assignments of the experimental vibrational frequencies are discussed in the cited literature.
[c] Relative to the energy sum of ground metal oxide and CH_3Cl.

Table 2. Ground electronic states, symmetry point groups, vibrational frequencies (cm^{-1}), and binding energies (kJ/mol) for the isomers of $MO(CH_3Cl)$ in solid argon[a].

The ground-state $NbO(CH_3Cl)$ and $TaO(CH_3Cl)$ molecules are related to the ground-state NbO ($^4\Sigma$) and TaO ($^2\Delta$). The predicted binding energies of 29.5 (Nb) and 5.0 kJ/mol (Ta) are larger than the corresponding values of $NbO(CH_4)$ and $TaO(CH_4)$ complexes [46], which were predicted to be very weakly interaction with the metal atom being bound to three hydrogen atoms of CH_4. The $MO(CH_3Cl)$ (M = Nb, Ta) complexes rearranged to the more stable doublet $CH_2ClM(O)H$ isomer upon visible light excitation, as shown in **Table 2**. Thus, some excited states may be involved during the reaction process. The $CH_2ClM(O)H$ molecules were predicted to involve agostic interactions between the chlorine atom and the metal center. It is quite interesting to note that the $CH_2ClM(O)H$ (M = Nb, Ta) molecules involve agostic interactions between the chlorine atom and the metal atom. It is notable that the group 5 metal methylidene complexes are more agostically distorted than the group 4 metal complexes.

Taking $CH_2ClNb(O)H$ as an example, the ∠ClCNb was predicted to be only 80.4° with a Cl—Nb distance of 2.624 Å. Agostic distortion interaction is a universal phenomenon in the structures of the early transition metal alkylidene complexes and even more popular in the structures of the small methylidene complexes, in which agostic interactions are also observed between the group 4–6 transition metal atom and one of the R-hydrogen atoms.

The reactions of FeO and MnO with CH_3Cl first formed the $MO(CH_3Cl)$ (M = Mn, Fe) complexes when annealing, which can isomerize to CH_3MOCl (M = Mn, Fe) upon $300 < \lambda < 580$ nm irradiation. The products were characterized by isotopic IR studies with CD_3Cl and $^{13}CH_3Cl$ and density functional calculations, as shown in **Figure 3**. Based on theoretical calculations, the $MO(CH_3Cl)$ (M = Mn, Fe) complexes have $^5A'$ for Fe and $^6A'$ ground state for Mn with C_s symmetry, respectively, as listed in **Table 1**. The binding energies of $MO(CH_3Cl)$ (M = Mn, Fe) are 9.3 and 23.3 kcal/mol lower than MO + CH_3Cl, which are higher in energy than $MO(CH_4)$ and MO(Ng) (Ng = Ar, Kr, Xe) at the same calculation level [46–48]. The accurate CCSD(T) single-point calculations illustrate the CH_3MOCl isomerism are 13.8 and 3.1 kcal/mol lower in energy than the $MO(CH_3Cl)$ (M = Mn, Fe) complexes.

The different reactivity of metal monoxide with CH_3Cl can be rationalized in terms of changes in valence electron structures accompanied by electronic spin state crossing. In the scandium and yttrium reactions, the ground ScO and YO molecules reacted with CH_3Cl to form two isomeric $MO(CH_3Cl)$ (M = Sc, Y) complexes spontaneously on annealing. Broad-band irradiation produced either the addition of the C—Cl bond to the O═M (M = Sc, Y) bond to form the CH_3OMCl (M = Sc, Y) molecules with +II oxidation state of center metal or the addition of the C—H bond to the M═O bond to give the CH_2ClMOH isomer with the valence of metal remaining in +II oxidation state. The CH_2ClMOH (M = Sc, Y) include one α-chlorine atom to form agostic molecules between chlorine atom and metal center atom with less than 90° of ∠ClCM and short Cl---M (M = Sc, Y) distances. No α-H and/or α-Cl atom for the $MO(CH_3Cl)$ complex exist, so no agostic interaction is observed. Sc and Y have only three valence electrons, and hence they are not able to form high oxidation state structures. However, Mn and Fe have five and six valence electrons. Because their d orbitals are fully half-filled and hence are not easily lost, upon $300 < k < 580$ nm irradiation the $MO(CH_3Cl)$ (M = Mn, Fe) complexes triggered the addition of the C—Cl bond to the M═O bond to form the CH_3MOCl molecules with +II valence state. The Ti and Zr metals have four valence electrons, and their oxidation states increase from +II to +IV during the addition of MO insertion into the C—Cl bond to the metal to form $CH_3M(O)Cl$ molecules. For Nb and Ta, visible light irradiation triggered the H-atom transfer of the $MO(CH_3Cl)$ complexes from CH_3Cl to the metal center to form the more stable $CH_2ClM(O)H$ isomers with the oxidation states of the metal increasing from the +II to +IV. However, the Nb and Ta have five valence electrons, and they cannot form +V oxidation structures, but possessing one valence electron characteristic of the agnostic chlorine effect.

4. Transition metal dioxides reaction with CH_3Cl

The ground-state MO_2 (M = Ti, Zr, Nb, Ta) molecules react with CH_3Cl to first form the weakly bound $MO_2(CH_3Cl)$ complexes with O···H and M···Cl bonds. For Ti and Zr, the $MO_2(CH_3Cl)$

http://dx.doi.org/10.5772/64437

complexes can isomerize to the more stable $CH_3OM(O)Cl$ molecules with the addition of the C—Cl bond of CH_3Cl to one of the O═M bond of MO_2 on annealing after broadband light irradiation ($\lambda < 300$ nm), as shown in **Figures 2** and **4**. And the reaction potential energy profile interpreted the chemical reaction mechanism of C—Cl activation by MO_2 (M = Ti, Zr). The photoisomerization reaction of $MO_2(CH_3Cl)$ (M = Nb, Ta) is quite different from those of $MO_2(CH_3Cl)$ (M = Ti, Zr). The $MO_2(CH_3Cl)$ (M = Nb, Ta) complexes were initiated H-transfer under ultraviolet light irradiation to isomerize the more stable $CH_2ClM(O)OH$ molecules. The $CH_2ClM(O)OH$ (M = Nb, Ta) molecules were predicted to involve agostic interactions between the chlorine atom and the metal center. During the photoisomerization process, no electronic spin state crossings were found, as shown in **Table 3**, different from the reaction of metal monoxides with CH_3Cl.

Molecule	Ground state	Point group	Vibrational frequency[b]	Binding energy[c]	Ref.
$TiO_2(CH_3Cl)$	^1A	C_1	940.3, 906.2	−95.7	[28]
$ZrO_2(CH_3Cl)$	$^1A'$	C_s	874.1, 804.2	−84.4	[28]
$NbO_2(CH_3Cl)$	^2A	C_1	948.1, 890.9	−75.66	[29]
$TaO_2(CH_3Cl)$	$^2A'$	C_s	948.4, 890.8	−52.9	[29]
$CH_3OTi(O)Cl$	^1A	C_1	1173.0, 1102.6, 634.1	−326.0	[28]
$CH_3OZr(O)Cl$	^1A	C_1	1153.1, 901.2	−331.9	[28]
$CH_2ClNb(O)OH$	^2A	C_1	3678.4, 979.4, 712.8	−185.5	[29]
$CH_2ClTa(O)OH$	^2A	C_1	3690.8, 975.9, 605.8, 495.7	−171.8	[29]

[a] Only the values for the most abundant metal isotope are listed.
[b] The mode assignments of the experimental vibrational frequencies are discussed in the cited literature.
[c] Relative to the energy sum of ground metal oxide and CH_3Cl.

Table 3. Ground electronic states, symmetry point groups, vibrational frequencies (cm^{-1}), and binding energies (kJ/mol) for the product from $MO_2 + CH_3Cl$ in solid argon[a].

5. Conclusion and outlook

C—Cl and/or C—H bond of monochloromethane activation by transition metal monoxide and dioxide molecules has been investigated using matrix infrared spectroscopy in excess argon and density functional theoretical calculations. The metal monoxide and dioxide molecules prepared by laser-ablated bulk higher oxide targets reacted with monochloromethane to form the weakly bound $MO(CH_3Cl)$ (x = 1, 2; M = Sc, Y, Nb, Ta, Ti, Zr, Mn, Fe) complexes, which

isomerized to the more stable CH_3OMCl (M = Sc, Y), agostic CH_2ClMOH (M = Sc, Y, Nb, Ta) and $CH_3M(O)Cl$ (M = Ti, Zr, Nb, Ta, Mn, Fe) isomers upon limited visible light excitation. Metal dioxides also reacted with CH_3Cl to form $MO_2(CH_3Cl)$ (M = Ti, Zr, Nb, Ta), which was rearranged to the more stable $CH_3OM(O)Cl$ (M = Ti, Zr) and $CH_2ClM(O)OH$ (M = Nb, Ta) molecules under ultraviolet light irradiation. Agostic interactions were observed in CH_2ClMOH (M = Sc, Y, Nb, Ta) and $CH_2ClM(O)OH$ (M = Nb, Ta) between the chlorine atom and the metal center atom.

Acknowledgements

We gratefully acknowledge the financial support from National Natural Science Foundation of China (Grants No. 21273202 and 21473162). Y. Zhao is grateful to the Project Grants 521 Talents Cultivation of Zhejiang Sci-Tech University and China Scholarship Council (CSC) Foundation. This work is also supported by Zhejiang Provincial Top Key Academic Discipline of Chemical Engineering and Technology.

Author details

Yanying Zhao[1,2*], Xin Liu[1] and Shuang Meng[1]

*Address all correspondence to: yyzhao@zstu.edu.cn

1 Department of Chemistry, Zhejiang Sci-Tech University, Hangzhou, China

2 State Key Laboratory of Advanced Textiles Materials and Manufacture Technology, MOE, Zhejiang Sci-Tech University, Hangzhou, China

References

[1] Yokouchi Y, Noijiri Y, Barrie LA, Toom-Sauntry D, Machida T, Inuzuka Y, Akimoto H, Li HJ, Fujinuma Y, Aoki SA. Strong source of methyl chloride to the atmosphere from tropical coastal land. Nature. 2000;403:295–298. DOI: 10.1038/35002049

[2] Yokouchi Y, Ikeda M, Inuzuka Y, Yukawa T. Strong emission of methyl chloride from tropical plants. Nature. 2002;416:163–165. DOI: 10.1038/416163a

[3] Tajima N, Tsuneda T, Toyama F, Hirao K. A new mechanism for the first carbon−carbon bond formation in the MTG process: a theoretical study. J. Am. Chem. Soc. 1998;120:8222–8229. DOI: 10.1021/ja9741483

[4] Hazari N, Lglesia E, Labinger JA, Simonetti, DA. Selective homogeneous and heterogeneous catalytic conversion of methanol/dimethyl ether to triptane. Acc. Chem. Res. 2012;45: 653–662. DOI: 10.1021/ar2002528

[5] Olah GA, Gupta B, Felberg JD, et al. Electrophilic reactions at single bonds. 20. Selective monohalogenation of methane over supported acid or platinum metal catalysts and hydrolysis of methyl halides over γ-alumina-supported metal oxide/hydroxide catalysts. A feasible path for the oxidative conversion of methane into methyl alcohol/dimethyl ether. J. Am. Chem. Soc. 1985;107:7097–7105. DOI: 10.1021/ja00310a057

[6] Olsbye U, Svelle S, Bjørgen M, Beato P, Janssens TVW, Joensen F, Bordiga S, Lillerud KP. Conversion of methanol to hydrocarbons: how zeolite cavity and pore size controls product selectivity. Angew. Chem. Int. Ed. 2012;51:5810–5831. DOI: 10.1002/anie.201103657

[7] Xu T, Zhang Q, Song H, Wang Y. Fluoride-treated H-ZSM-5 as a highly selective and stable catalyst for the production of propylene from methyl halides. J. Catal. 2012;295:232–241. DOI: 10.1016/j.jcat.2012.08.014

[8] Zhang R, Zhang B, Shi Z, Liu N, Chen B. Catalytic behaviors of chloromethane combustion over the metal-modified ZSM-5 zeolites with diverse SiO_2/Al_2O_3 ratios. J. Mol. Catal. A: Chem. 2015;398:223–230. DOI: 10.1016/j.molcata.2014.11.019

[9] Kong L, Shen B, Zhao J, Liu J. Comparative study on the chloromethane to olefins reaction over SAPO-34 and HZSM-22. Ind. Eng. Chem. Res. 2014;53:16324–16331. DOI: 10.1021/ie5028155

[10] Olsbye U, Saure OV, Muddada NB, Bordiga S, Lamberti C, Nilsen M H, Lillerud KP, Svelle S. Methane conversion to light olefins – how does the methyl halide route differ from the methanol to olefins (MTO) route? Catal. Today. 2011;171:211–220. DOI: 10.1016/j.cattod.2011.04.020

[11] Wei Y, Zhang D, Chang F, Xia Q, Su BL, Liu Z. Ultra-short contact time conversion of chloromethane to olefins over precoked SAPO-34: direct insight into the primary conversion with coke deposition. Chem. Commun. 2009;40:5999–60001. DOI: 10.1039/b909218h

[12] Xu L, Du AP, Wei YX. Synthesis of SAPO-34 with only Si(4Al) species: effect of Si contents on Si incorporation mechanism and Si coordination environment of SAPO-34. Micropor. Mesopor. Mater. 2008;115:332–337. DOI: 10.1016/j.micromeso.2008.02.001

[13] Jiang Z, Shen B, Zhao J, Wang L, Kong L, Xiao W. Enhancement of catalytic performances for the conversion of chloromethane to light olefins over SAPO-34 by modification with metal chloride. Ind. Eng. Chem. Res. 2015;54(49):12293–12302. DOI: 10.1021/acs.iecr.5b03586

[14] Yang CT, Zhang ZQ, Liang J, Liu JH, Lu XY, Chen HH, Liu L. Copper-catalyzed cross-coupling of nonactivated secondary alkyl halides and tosylates with

secondary alkyl Grignard reagents. J. Am. Chem. Soc. 2012;134:11124–11127. DOI: 10.1021/ja304848n

[15] Rudolph A, Lautens M. Secondary alkyl halides in transition metal-catalyzed cross-coupling reactions. Angew. Chem. Int. Ed. 2009;48:2656–2670. DOI: 10.1002/anie.200803611

[16] Xiao B, Liu ZJ, Liu L, Fu Y. Palladium-catalyzed C–H activation/cross-coupling of pyridine N-oxides with nonactivated secondary alkyl bromides. J. Am. Chem. Soc. 2013;135:616–619. DOI: 10.1021/ja3113752

[17] Cho HG, Andrews L. Persistent photo-reversible transition-metal methylidene system generated from reaction of methyl fluoride with laser-ablated zirconium atoms and isolated in a solid argon matrix. J. Am. Chem. Soc. 2004;126(33):10485–10492. DOI: 10.1021/ja0486115

[18] Cho HG, Andrews L. Infrared spectra of CH_3–MX and CH_2X–MH prepared in reactions of laser-ablated gold, platinum, palladium, and nickel atoms with CH_3Cl and CH_3Br. Organometallics. 2013;32(9):2753–2759. DOI: 10.1021/om400192v

[19] Cho HG, Andrews L. Infrared spectra of CX_3—MnX and CX_2═MnX_2 (X = H, F, Cl) prepared in reactions of laser-ablated manganese atoms with halomethanes. Organometallics. 2011;30(3):477–486. DOI: 10.1021/om100791h

[20] Cho HG, Andrews L. Infrared spectra of simple methylidyne, methylidene, and insertion complexes generated in reactions of laser-ablated rhodium atoms with halomethanes and ethane. Organometallics. 2010;29(10):2211–2222. DOI: 10.1021/om900902p

[21] Cho HG, Andrews L. Infrared spectra of the CH_3—MX, $CHMH_2X$— complexes formed by reaction of methyl halides with laser-ablated group 5 metal atoms. J. Phys. Chem. A. 2006;110:10063–10077. DOI: 10.1021/jp0629644

[22] Cho HG, Andrews L. Infrared spectra of the CH_3—MX and CH_2—MHX complexes formed by reactions of laser-ablated group 3 metal atoms with methyl halides. J. Phys. Chem. A. 2007;111:2480–2491. DOI: 10.1021/jp067662g

[23] Cho HG, Andrews L. Formation of CH_3TiX, CH_2═TiHX, and $(CH_3)_2TiX_2$ by reaction of methyl chloride and bromide with laser-ablated titanium atoms: photoreversible α-hydrogen migration. Inorg. Chem. 2005;44(4):979–988. DOI: 10.1021/ic048615a

[24] Cho HG, Andrews L. Infrared spectra of methylidynes formed in reactions of Re atoms with methane, methyl halides, methylene halides, and ethane: methylidyne C—H stretching absorptions, bond lengths, and s character. Inorg. Chem. 2008;47:1653–1662. DOI: 10.1021/ic701505w

[25] Cho HG, Andrews L. Infrared spectra of platinum insertion and methylidene complexes prepared in oxidative C—H(X) reactions of laser-ablated pt atoms with methane,

ethane, and halomethanes. Organometallics. 2009;28:1358–1368. DOI: 10.1021/om801077x

[26] Jonathan TL, Cho HG, Andrews L. Methylidyne XC ⋮ MX_3 (M = Cr, Mo, W; X = H, F, Cl) diagnostic C—H and C—X stretching absorptions and methylidene CH_2═MX_2 analogues. Organometallics. 2007;26(25):6373–6387. DOI: 10.1021/om700689e

[27] Zhao Y. C–Cl activation by group IV metal oxides in solid argon matrixes: matrix isolation infrared spectroscopy and theoretical investigations of the reactions of MO_x (M = Ti, Zr; x = 1, 2) with CH_3Cl. J. Phys. Chem. A. 2013;117(27):5664–5674.

[28] Zhao Y, Huang Y, Zheng X, Zhou M. Preparation and characterization of the agostic bonding molecules between metal and chlorine from the reactions of niobium and tantalum monoxide and dioxide molecules with monochloromethane in solid argon. J. Phys. Chem. A. 2010;114(18):5779–5786. DOI: 10.1021/jp102199c

[29] Huang Y, Zhao Y, Zheng X, Zhou M. Matrix isolation infrared spectroscopic and density functional theoretical study of the reactions of scandium and yttrium monoxides with monochloromethane. J. Phys. Chem. A. 2010;114(7):1476–2482. DOI: 10.1021/jp9101948

[30] Zhao Y, Fan K, Huang Y, Zheng X. Matrix isolation infrared spectra, assignment and DFT investigation on reactions of iron and manganese monoxides with CH_3Cl. Spectrochim. Acta A Mol. Biomol. Spectrosc. 2013;116:96–101. DOI: 10.1016/j.saa.2013.07.010

[31] Gong Y, Zhou M, Andrews L. Spectroscopic and theoretical studies of transition metal oxides and dioxygen complexes. Chem. Rev. 2009;109(12): 6765–6808. DOI: 10.1021/cr900185x

[32] Zhao Y, Gong Y, Chen M, Zhou M. Noble gas-transition-metal complexes: coordination of VO_2 and VO_4 by Ar and Xe atoms in solid noble gas matrixes. J. Phys. Chem. A. 2006;110(5):1845–1849. DOI: 10.1021/jp056476s

[33] Wang C, Zhuang J, Wang G, Chen M, Zhao Y, Zheng X, Zhou M. Tantalum dioxide complexes with dinitrogen. Formation and characterization of the side-on and end-on bonded $TaO_2(NN)_x$ (x = 1–3) complexes. J. Phys. Chem. A. 2010;114(31):8083–8089. DOI: 10.1021/jp103866r

[34] Zhao Y, Gong Y, Chen M, Ding C, Zhou M. Coordination of ScO^+ and YO^+ by multiple Ar, Kr, and Xe atoms in noble gas matrixes: a matrix isolation infrared spectroscopic and theoretical study. J. Phys. Chem. A. 2005;109(51):11765–11770. DOI: 10.1021/jp054517e

[35] Frisch MJ, Trucks GW, Schlegel HB, Scuseria GE, Robb MA, Cheeseman JR, Montgomery JA, Vreven T, Kudin KN, Burant JC, Millam JM, Iyengar SS, Tomasi J, Barone V, Mennucci B, Cossi M, Scalmani G, Rega N, Petersson GA, Nakatsuji H, Hada M, Ehara M, Toyota K, Fukuda R, Hasegawa J, Ishida M, Nakajima T, Honda Y, Kitao O, Nakai H, Klene M, Li X, Knox JE, Hratchian HP, Cross JB, Adamo C, Jaramillo J, Gomperts R, Stratmann RE, Yazyev O, Austin AJ, Cammi R, Pomelli C, Ochterski JW, Ayala PY,

Morokuma K, Voth GA, Salvador P, Dannenberg JJ, Zakrzewski VG, Dapprich S, Daniels AD, Strain MC, Farkas O, Malick DK, Rabuck AD, Raghavachari K, Foresman JB, Ortiz JV, Cui Q, Baboul AG, Clifford S, Cioslowski J, Stefanov BB, Liu G, Liashenko A, Piskorz P, Komaromi I, Martin RL, Fox DJ, Keith T, Al-Laham MA, Peng CY, Nanayakkara A, Challacombe M, Gill PMW, Johnson B, Chen W, Wong MW, Gonzalez C, Pople JA. Gaussian 03, Revision B.05, Gaussian. Inc.: Pittsburgh, PA, 2003.

[36] Becke AD. Density-functional thermochemistry. III. The role of exact exchange. J. Chem. Phys. 1993;98:5648–5652. DOI: 10.1063/1.464913

[37] Lee C, Yang W, Parr RG. Development of the Colle–Salvetti correlation-energy formula into a functional of the electron density. Phys. Rev. B. 1988;B37:785–789. DOI: 10.1103/PhysRevB.37.785

[38] McLean AD, Chandler GS. Contracted Gaussian basis sets for molecular calculations. I. Second row atoms, Z = 11 − 18. J. Chem. Phys. 1980;72:5639–5648. DOI: 10.1063/1.438980

[39] Krishnan R, Binkley JS, Seeger R, Pople JA. Self-consistent molecular orbital methods. XX. A basis set for correlated wave functions. J. Chem. Phys. 1980;72:650–654. DOI: 10.1063/1.438980

[40] Godbout N, Salahub DR, Andzelm J, Wimmer E. Optimization of Gaussian-type basis sets for local spin density functional calculations. Part I. Boron through Neon, optimization technique and validation. Can. J. Chem. 1992;70:560−571. DOI: 10.1139/v92-079

[41] Sosa C, Andzelm BC, Wimmer E, Dobbs KD, Dixon DA. A local density functional study of the structure and vibrational frequencies of molecular transition-metal compounds. J. Phys. Chem. 1992;96:6630–6636. DOI: 10.1021/j100195a022

[42] Dolg M, Stoll H, Preuss H. Energy-adjusted abinitio pseudopotentials for the rare earth elements. J. Chem. Phys. 1989;90(3):1730–1734. DOI: 10.1063/1.456066

[43] Andrae D, Haeussermann U, Dolg M, Stoll H, Preuss H. Energy-adjusted *ab initio* pseudopotentials for the second and third row transition elements. J. Theor. Chim. Acta, 1990;77(2):123–141. DOI:10.1007/BF01114537

[44] Pople JA, Head-Gordon M, Raghavachari K. Quadratic configuration interaction. a general technique for determining electron correlation energies. J. Chem. Phys. 1987;87:5968–5975. DOI: 10.1063/1.453520

[45] Wang G, Gong Y, Chen M, Zhou M. Methane activation by titanium monoxide molecules: a matrix isolation infrared spectroscopic and theoretical study. J. Am. Chem. Soc. 2006;128(17):5974–5980. DOI: 10.1021/ja0604010

[46] Wang G, Zhou M. Probing the intermediates in the $MO + CH_4 \leftrightarrow M + CH_3OH$ reactions by matrix isolation infrared spectroscopy. Int. Rev. Phys. Chem. 2008;27(1):1–25. DOI: 10.1080/01442350701685946

[47] Zhao Y, Gong Y, Zhou M. Matrix isolation infrared spectroscopic and theoretical study of NgMO (Ng = Ar, Kr, Xe; M = Cr, Mn, Fe, Co, Ni) complexes. J. Phys. Chem. A. 2006;110(37):10777–10782. DOI: 10.1021/jp064100o

[48] Zhao Y, Zhou M. Are matrix isolated species really "isolated"? Infrared spectroscopic and theoretical studies of noble gas-transition metal oxide complexes. Sci. China Chem. 2010;53(2):327–336. DOI: 10.1007/s11426-010-0044-9

IntechOpen

IntechOpen